Interpretation of gravity and magnetic anomalies at Lake Rotomahana: geological and hydrothermal implications

F. Caratori Tontini[a*], C.E.J. de Ronde[a], B.J. Scott[b], S. Soengkono[b], V. Stagpoole[a], C. Timm[a], M. Tivey[c]

[a] GNS Science, 1 Fairway Dr, Lower Hutt 5010, New Zealand
[b] GNS Science, 114 Karetoto Road, RD4, Taupo 3384, New Zealand
[c] Woods Hole Oceanographic Institution, 266 Woods Hole Rd., Woods Hole, MA 02543, USA

Keywords: Lake Rotomahana; hydrothermal systems; magnetic anomalies; gravity anomalies; phreatomagmatic eruptions; basaltic dikes.

[*] Corresponding author: Fabio Caratori Tontini
GNS Science
1 Fairway dr
Lower Hutt 5010
New Zealand
Tel: +64 4 5704760
Email: f.caratori.tontini@gns.cri.nz

ABSTRACT

We investigate the geological and hydrothermal setting at Lake Rotomahana, using recently collected potential-field data, integrated with pre-existing regional gravity and aeromagnetic compilations. The lake is located on the southwest margin of the Okataina Volcanic Center (Haroharo caldera) and had well-known, pre-1886 Tarawera eruption hydrothermal manifestations (the famous Pink and White Terraces). Its present physiography was set by the caldera collapse during the 1886 eruption, together with the appearance of surface activities at the Waimangu Valley. Gravity models suggest subsidence associated with the Haroharo caldera is wider than the previously mapped extent of the caldera margins. Magnetic anomalies closely correlate with heat-flux data and surface hydrothermal manifestations and indicate that the west and northwestern shore of Lake Rotomahana are characterized by a large, well-developed hydrothermal field. The field extends beyond the lake area with deep connections to the Waimangu area to the south. On the south, the contact between hydrothermally demagnetized and magnetized rocks strikes along a structural lineament with high heat-flux and bubble plumes which suggest hydrothermal activity occurring west of Patiti Island. The absence of a well-defined demagnetization anomaly at this location suggests a very young age for the underlying geothermal system which was likely generated by the 1886 Tarawera eruption. Locally confined intense magnetic anomalies on the north shore of Lake Rotomahana are interpreted as basalts dikes with high magnetization. Some appear to have been emplaced before the 1886 Tarawera eruption. A dike located in proximity of the southwest lake shore may be related to the structural lineament controlling the development of the Patiti geothermal system, and could have been originated from the 1886 Tarawera eruption.

1. Introduction

Lake Rotomahana (LR) is one of many volcanic lakes in the Rotorua District (Healy 1975a), within the Taupo Volcanic Zone (TVZ) on the North Island of New Zealand (Fig.1). It is located approximately 1 km south of Lake Tarawera (LT) and 5 km southwest of Tarawera Volcanic Complex (TVC). The active Waimangu Valley (WV) is the southwest extension of Lake Rotomahana thermal area. On the 10th of June 1886, a devastating explosive eruption formed a 17 km long chain of craters, from Mt Tarawera through the former smaller Lake Rotomahana to the Waimangu Valley area (Fig.1), which is known as the 1886 Tarawera Rift eruption. This eruption was a short, powerful basaltic fissure eruption that ended with a phreatomagmatic explosion at Rotomahana and Waimangu, where several craters in alignment with Tarawera fissure trend were formed independently of topography (e.g., Cole, 1970; Nairn, 1979; Nairn and Cole, 1981, Nairn 2002).

Modern Lake Rotomahana currently lays within a series of deep interconnected craters (Nairn 1979) that were formed during the Tarawera Rift eruption. Before 1886, two smaller lakes (Lake Rotomahana and Lake Rotomakariri) were located in this area (Fig.2). The pre-1886 smaller Lake Rotomahana had well-known hydrothermal activities, such as the Pink and White Terraces on the western side (Hochstetter, 1864). Following the landscape changing 1886 eruption water ponded in the craters and the level rose due to climate and rainfall (Healy 1975b), now covering an area of ~ 8 km^2 and a maximum depth of ~ 130 m (Keam, 1988).

The 1886 Tarawera Rift is part of the Okataina Volcanic Center (OVC), delimited by a major caldera, forming one of at least four major volcanic centres in the TVZ (Wilson et al., 1984). The lake area lays in a collapse embayment in the south western portion of the Okataina Volcanic Centre (OVC), where the Haroharo Caldera boundaries are poorly defined (Nairn 2002). Geothermal activity is widespread in the Lake Rotomahana area occurring along the northwestern and southern lake shores, in the Waimangu Valley, north of the lake on the divide with Lake Tarawera and in the Haumi Stream to the south. Bubbles and plumes of hot water are also observed in the lake (Fig. 2). All these geothermal manifestations are part of the Waimangu-Rotomahana- Mt Tarawera Geothermal Field.

In this study, we will show the interpretation of new gravity and magnetic data collected at Lake Rotomahana in 2011 and integrated with pre-existing aeromagnetic data. We will analyse these data to identify the extent and subsurface distribution of hydrothermal alteration and investigate the distribution of volcanic rocks under the lake floor.

2. Geological and geothermal setting

Lake Rotomahana is located in a topographic low formed by the collapse of the southwestern edge of the Haroharo Caldera (Nairn, 1981; Rogan, 1982; Wilson et al., 1984; Nairn 2002). The Okataina Volcanic Centre is characterized by a major negative gravity anomaly (Rogan, 1982; Seebeck et al., 2010). Joint gravity and magnetic modelling suggest a depth to the greywacke basement up to 5 km under the Okataina Volcanic Centre (Haroharo caldera) with a shallow, 1-2 km thick layer of magnetized rocks (Rogan, 1982), suggesting the existence of a deep felsic magma body with temperature still above the Curie point. Basement rocks become shallower on all sides of the caldera and in the Rotomahana area (Fig. 2) the basement depth is shallower than 500 m (Rogan, 1982), almost outcropping under Lake Rotomahana and along the south shore of Lake Tarawera.

The erupted material around Lake Rotomahana and Mt Tarawera is mainly rhyolitic (Wilson et al., 1984; Nairn and Cole, 1981; Nairn, 2002) being part of four major eruptive episodes building the Tarawera Volcanic Complex since 17000 years ago (Cole, 1970; Nairn, 1981; Nairn, 2002). There is evidence of basalt erupted during each of these rhyolite episodes (Nairn, 1992, 2002; Darragh et al., 2006; Shane et al., 2007) and it is believed that injections of basaltic magma played a key role in triggering the rhyolitic eruptions (Villamor et al., 2007; Leonard et al., 2002). Basalts predating the 1886 eruption (Nairn, 1979; Nairn and Cole, 1981) have been mapped along the South and North shore of Lake Rotomahana (Fig.2). The rocks in the study area (Fig. 2) are normally magnetized lavas and ignimbrites younger than 0.3 Ma (Soengkono, 2001; Leonard et al., 2010).

The 1886 Tarawera Rift eruption was characterized by the intrusion of basaltic dikes along a 17 km long rift dissecting the original Tarawera rhyolite massif, forming a series of separate and coalescing explosion craters (Nairn, 1979; Nairn and Cole, 1981). Although Mt. Tarawera is a rhyolitic volcano, the 1886 eruption produced basaltic scoria and lavas. Basaltic dikes reaching the groundwater led to a series of phreatomagmatic and hydrothermal explosions extending from Mt. Tarawera to the Waimangu Valley, crossing Lake Rotomahana in between (Nairn, 1979; Nairn, 2002; Nairn and Cole, 1981; Walker et al., 1984). Today these dikes appear 1-20 m wide (Cole and Hunt, 1968; Rogan and Hochstein, 1984), but are preserved only in a few places (Nairn and Cole, 1981). In particular, 1886 basalt was erupted at Echo Crater and Black Crater in the Waimangu Valley, at all the Tarawera Craters, and probably at Lake Rotomahana (Nairn, 1981).

The 1886 eruption generated new geothermal activity along the Waimangu Valley, by creating new conduits for both discharge and recharge zones (Simmons et al., 1993). A powerful geyser was active in the area from 1900 up to 1904 (Keam, 1988). The Waimangu portion of the Waimangu-Rotomahana-Mt Tarawera Geothermal Field is characterized by intense surface manifestations such as boiling springs, thermal pools and hot mud pools. Lake Rotomahana was already a very active surface hydrothermal field before the 1886 eruption (Hochstetter, 1864). However, the 1886 eruption changed the surface expression of the hydrothermal system in the area, by excavating deep craters, destroying parts of the famous Pink and White Terraces and enlarging the Lake Rotomahana basin. Today, hydrothermal plumes at Lake Rotomahana (Fig. 2) are mainly concentrated on the northwest shore of the lake (Pink Terraces hydrothermal system) and to the south along a linear feature west of Patiti Island (Patiti hydrothermal system) (Whiteford and Graham, 1995).

3. Methods and data

The results shown in this paper are mainly based on potential-field modelling using pre-existing gravity (Stern, 1979; Stagpoole and Bibby, 1999; Seebeck et al., 2010) and aeromagnetic (Soengkono, 2001) data. In 2010 we collected 20 new gravity stations and integrated them into the pre-existing GNS Science gravity database. In addition, a high-resolution magnetic survey was conducted at Lake Rotomahana in 2010 to explore shallow geological features under the lake floor.

3.1 Gravity data

Residual gravity data can be used to estimate the thickness of the caldera infill because of a negative density contrast (-0.5 g/cm^3) between the greywacke basement and the volcanoclastic infill (Stern, 1979; Rogan, 1982; Stern, 1986; Stagpoole, 1994; Stagpoole and Bibby, 1999; Seebeck et al., 2010). In our particular case, gravity modelling can produce a reasonable estimate for the Okataina Volcanic Centre (Haroharo caldera) margin in the Lake Rotomahana area.

The residual gravity map is shown in Fig. 3a. This map was compiled by using 37 pre-existing gravity stations from the New Zealand Land Gravity Database and from Seebeck et al. (2010) and by adding 20 new gravity measurements that we collected in 2011 using a Lacoste and Romberg G meter. These new data were tied to the New Zealand Primary Gravity Network (Reilly, 1972) and processed by using a reference density of 2.67 g/cm^3 for Bouguer and Terrain corrections (Caratori Tontini et al., 2007). The residual gravity anomaly was calculated by subtracting a regional gravity field obtained by a third-order polynomial expansion of the Bouguer gravity anomaly at locations where the greywacke basement outcrops (Stern, 1979; Stagpoole and Bibby, 1999).

3.2 Aeromagnetic data

Magnetic anomalies are useful in the delineation of high-temperature hydrothermal/geothermal systems because hydrothermal processes can significantly reduce the rock magnetization either through thermal demagnetization or by the alteration of magnetic minerals to less magnetic minerals (e.g., Tivey and Dyment, 2010; Caratori Tontini et al., 2012a; Caratori Tontini et al., 2010; Hochstein and Soengkono, 1997). Temperatures inside a geothermal reservoir do not exceed the 580° Curie temperature of magnetite (Carmichael, 1982), but hydrothermal alteration can dissolve and/or replace magnetic minerals, such as magnetite, into less magnetic minerals such as maghemite and pyrite, thus demagnetizing the host rocks (e.g. Lindgren, 1933; Ade-Hall et al., 1971; Rona, 1978; Johnson et al., 1982; Auerbach and Bleil, 1987).

Aeromagnetic data in the TVZ also support the presence of felsic magma chambers beneath the volcanic centres and in particular at the Okataina Volcanic Centre (Rogan, 1982). Gravity alone cannot distinguish between volcanoclastic infill and felsic magma because they both produce negative gravity anomalies. However, felsic magma has no remanent magnetization because the temperature exceeds the Curie temperature for magnetite (Carmichael, 1982).

The total magnetic intensity (TMI) aeromagnetic anomalies in the area of study are shown in Fig. 3b (Soengkono, 2001). The data were collected along North-South trending lines, with 1 km average line-spacing, at an average altitude of 350 m above the ground. Diurnal correction was applied by using a base-station magnetometer installed near Rotorua airport during the survey (Soengkono, 2001). The magnetic data were processed by subtracting the International Geomagnetic Reference Field (IGRF) model (e.g., Finlay et al., 2010) and a long-wavelength regional field describing the contribution of deep magnetic bodies (Soengkono, 1995).

3.3 Lake magnetic survey

High-resolution magnetic data were collected on Lake Rotomahana in February 2011 along the NW-SE oriented survey lines shown in Fig. 4a, spaced ~100 m apart with perpendicular control tie-lines spaced 250 m apart. The line orientation was chosen to perpendicularly cross the main structural lineament of the 1886 Tarawera Rift. The data were collected using a Marine Magnetics Seaspy magnetometer towed 20 m behind the stern of the Waikato University aluminium (non-magnetic) survey boat. The location of the magnetic sensor was determined by differential GPS data. Diurnal variation of the magnetic field was monitored using data from Eyrewell Intermagnet observatory (e.g., Faggioni and Caratori Tontini, 2002). The TMI anomaly field was obtained by subtraction of the IGRF model (e.g., Finlay et al., 2010) and the regional field of Soengkono (1995).

The accuracy of the survey can be assessed by analysing the cross-over error distribution, i.e., the difference in magnetic anomalies at the crossing points between survey lines and control tie-lines. The Lake Rotomahana survey is characterized by 203 crossing points and the average difference at the crossing points is -0.3 nT. The analysis shows very good-quality data, as the cross-over errors do not exceed 20 nT and have a standard deviation of 10 nT, which is less than 1% of the magnetic anomaly data amplitude (1300 nT). Furthermore, cross-over errors are normally distributed with no significant correlation pattern in time, demonstrating that there is no significant contribution from diurnal variation of the Earth magnetic field in the residual data.

4. Potential-field data modelling and interpretation

Quantitative interpretation of gravity and magnetic data at Lake Rotomahana provides information about the density and magnetization models in the study area. These models are correlated with pre-existing geological information to constrain the shape of the caldera boundary and the distribution of fresh volcanic rocks and hydrothermally altered rocks in the area of Lake Rotomahana.

4.1 Gravity data forward modelling

Simple 2D gravity models can help to estimate the depth of the basement as defined by density and the geometry of faults and caldera margins (e.g., Rogan, 1982; Stagpoole, 1994; Davy and

Caldwell, 1998; Davy and Bibby, 2005; Seebeck et al., 2010). To this aim we have evaluated two gravity models (Fig. 5a, 5b) along the profiles shown in Fig. 5c, using the 2.5D forward modeling Geosoft GmSys software. The models are based on a simple two-layer density distribution and assume a density contrast of -0.5 g/cm^3 between the top layer (volcanic infill) and the bottom layer (basement/greywacke). This density contrast derives from a mean density value of 2.67 g/cm^3 for the basement/greywacke and 2.17 g/cm^3 for the volcanic infill. These values are in agreement with density measurements on existing samples for the volcanic infill (Rogan, 1982) and the greywacke (Hatherton and Leopard, 1964). Furthermore, a density contrast of -0.5 g/cm^3 was used in previous gravity studies in the TVZ (Rogan, 1982; Malahoff, 1968; Hochstein and Hunt, 1970). The depth of the basement interface is estimated by fitting the observed gravity profile extracted from the Bouguer residual gravity map in Fig. 3a.

4.2 Magnetic data inversion

Inversion of magnetic data is a mathematical operation aimed at obtaining a subsurface 3-D magnetization distribution which reproduces the magnetic observations within some degree of accuracy (e.g., Blakely, 1995; Silva et al., 2001; Caratori Tontini et al., 2003). The equivalent magnetization distribution can be interpreted to obtain information about the distribution of fresh volcanic rocks (strongly magnetized) and the geometry of weakly magnetized hydrothermally altered rocks (e.g., Tivey and Johnson, 2002; Caratori Tontini et al., 2012b, Caratori Tontini et al., 2013).

The inverse model is commonly parameterized by subdividing the Earth’s subsurface by using a 3-D grid of smaller cells with uniform and constant magnetization. The inversion process is based on the estimate of the magnetization of each cell and complex magnetization distributions reproducing the observations are thus obtained. This problem is characterized by non-uniqueness and ambiguities of the solutions, i.e., a large number of solutions may fit the data with the same degree of accuracy.

A common practice to reduce these ambiguities is through regularization of the inversion itself, i.e., by introducing constraints about the source geometry and the magnetization parameters in the inversion process. In this particular case, we obtain a magnetization distribution which reproduces the observed data and is subject to geological constraints regarding the shape of the magnetization distribution and the range of the magnetization parameters. We have applied the inversion method of Caratori Tontini et al. (2012b) both to the aeromagnetic data (Fig. 3b) and to the lake magnetic data (Fig. 4b) as this method has proven very useful in mapping the 3-D distribution of hydrothermal alteration and volcanic rocks. The mathematical approach is described in detail in Caratori Tontini et al., (2012b), but we summarize the main constraints here:

- Given the young age of the volcanic rocks, the direction of the magnetization is assumed to be constant and parallel to the ambient geomagnetic field, which is determined by the IGRF model (Finlay et al., 2010). In the study area magnetic inclination is -60° while the declination is 20° E. This assumption is also justified by the paleomagnetic analysis of representative rock samples (Cox, 1971);

- Magnetization values are bounded in the range [0; 2.5] A/m, i.e., lower and upper bounds are imposed on the magnetization values. The lower bound is justified by the fact that the last magnetic reversal predates the commencement of volcanism in the study area (Wilson et al., 1985), and there is no known reversely (negative) magnetized rocks in the study area (Soengkono, 2001). The upper bound is based on the average magnetization of rhyolite in the TVZ which is ~2.5 A/m (Rogan, 1982; Soengkono, 2001);
- A sharp, focused solution is obtained by minimizing the volumes of the regions where the magnetization distribution gradients are larger than a small threshold value. This constraint is particularly effective at mapping regions of hydrothermal alteration because sharp contacts are expected between hydrothermally altered rocks and fresh volcanic rocks in upflow zones (Caratori Tontini et al., 2012b).

The resulting 3-D models based on the interpretation of the inversion results are shown in Fig. 6 for the regional aeromagnetic data and Fig. 7 for the lake magnetic data, respectively.

5. Discussion

Gravity modelling along the two sections in Fig. 5 show evidence of steep slopes or offsets in the boundaries between the volcanic infill and denser basement material below. The points marked by A, B, C, and D may be used to estimate the geometry and boundaries of the southern Okataina caldera margin in the Lake Rotomahana area. In particular, lines AC and BD in Fig. 5c show the gravity expression of the caldera margins, defining a depression trending SW-NE to the caldera edge. The basement steps down from the SE and NW into the Rotomahana basin (Fig. 5a, b). These margins are different to the mapped topographic margins inferred by Nairn (2002). The southwestern extent of this depression is overlain by the younger Rotomahana-Hapeotoroa lava domes and suggests ~ 1 km northern and southern extensions of the subsidence associated with the caldera collapse. The SW-NE structural trend associated with the gravity boundary (lines AC and BD) is also visible in the orientation of two positive ridges in the regional aeromagnetic map of Fig.3b, parallel to the 1886 Tarawera rift direction. This feature may also align with the eastern margin of the TVZ as modelled by Stagpoole (1994) along the edge of the Reporoa Caldera, 20 km south of Lake Rotomahana.

Two pronounced magnetic lows are located to the Northeast of Lake Rotomahana, south of Mt. Tarawera and North northwest of the Waimangu Valley (Fig. 3b). Magnetic modelling of terrain (Soengkono, 2001) show weak negative effects in these areas, but these effects are too low to explain the observed intense negative anomalies. Given these anomalies lie outside of the low-resistivity boundary of Bibby et al. (1994), the more likely explanation is that these negative anomalies are caused by buried reversely magnetized rocks. The objective of this paper however is to interpret anomalies that are more likely associated with geothermal systems. In this context, the regional aeromagnetic map (Fig. 3b) also provides evidence of a magnetic low on the western side of Lake Rotomahana, coalescing into a broader magnetic low extending southwest into the Waimangu Valley area. The boundary of this broad low magnetic anomaly is roughly coincident with a low-resistivity expression of the Waimangu-Rotomahana-Mt Tarawera geothermal field boundary (Bibby et al., 1994) and encloses the fault interpreted as a permeable pathway for aqueous fluid and CO2 release by Bannister et al. (this volume). The lake magnetic anomaly map in Fig. 4b clearly shows a pronounced low on the western and northwestern shore of Lake Rotomahana, where the uppermost part of the deeper conductive zone is located (Heise et al., this volume). The shape of this magnetic anomaly shows a very good correlation with recently collected heat-flow data (Tivey et al., this volume) and hydrothermal plumes (de Ronde et al., this volume; Mazot et al., 2014), reinforcing the geothermal origin for this anomaly.

Under the assumption that hydrothermal activity results in complete demagnetization, the 3-D rock magnetization model in Fig. 6 can be used to interpret the subsurface distribution of hydrothermally altered rocks. This model, based on the inversion of regional aeromagnetic data, shows a large demagnetized body located under the Waimangu portion of the Waimangu-Rotomahana-Mt Tarawera geothermal field, whose eastern boundary lies under the western side of Lake Rotomahana. These results are in good agreement with the magnetic analysis of Soengkono (2001), but provide additional evidence for the presence of demagnetized rocks beneath the western side of Lake Rotomahana.

The size and shape of the demagnetized body indicates a deep, well-established connection between the Waimangu portion of the Waimangu-Rotomahana-Mt Tarawera geothermal field and the geothermal manifestations on the western side of Lake Rotomahana (Pink Terraces hydrothermal system). Furthermore, the horizontal shape of the demagnetized region is consistent with the resistivity boundary of Bibby et al. (1994), confirming that the subsurface distribution of the Waimangu system is larger than the surface geothermal area (Soengkono, 2001).

The 3-D model in Fig. 6 also suggests a gradual thickening of the distribution of the subsurface geothermal system along a southwest-northeast trend, with a ~1000 m thick layer of demagnetized rocks just under the area southwest of the Waimangu Thermal Area gradually thinning to ~400 m beneath the western corner of Lake Rotomahana. This suggests that geothermal system manifestations under the Waimangu Valley and under Lake Rotomahana area could be of significant age, sourced west of the major upflow paths at Rotomahana and could be due to a single, deep geothermal plume located under Waimangu. This deep connection is believed active before the 1886 eruption with the Rotomahana-Rotomahana-Mt Tarawera hydrothermal system near a steady state of activity (Simmons, 1983).

This seems to disagree with the fact that there was little, to no reported surface geothermal manifestations in the Waimangu Valley prior to the eruption (Keam, this issue). It is possible that if an active geothermal field was present before the eruption it was likely below ground surface. Furthermore, the plan-view of the demagnetized region is consistent with the resistivity boundary of Bibby et al. (1994), confirming that the subsurface distribution of the Waimangu geothermal field may be larger than the surface geothermal area (Soengkono, 2001). The magnetic method however can be used to map extinct fields as hydrothermal alteration and rock demagnetization persists even after the termination of geothermal activity (Caratori Tontini et al., 2012a). Another possible explanation is that the significant volume of demagnetized rocks beneath Waimangu is related to the presence of an old geothermal system which was very active well before 1886 and geothermal activity was waning down at the time of the 1886 eruption. This may also explain why the rift went through the Waimangu valley as hydrothermally altered rocks are inherently weak and permeable to the dikes injection.

A detailed 3-D magnetic model of Lake Rotomahana, based on the high-resolution lake magnetic survey is shown in Fig. 7. Heat-flow observations (Tivey et al., this volume) and hydrothermal plumes (de Ronde et al., this volume, Walker et al., this volume) are in agreement with the shape of the demagnetized body, confirming hydrothermal alteration as the most likely explanation for the zones of low magnetization at the Pink Terraces hydrothermal system. The maximum observed heat-flow values [10-40 W/m^2] are found in this region and the boundary of the demagnetized body approximately follows the 2 W/m^2 contour line in the heat-flow map of Tivey et al., (this volume).

The area of the Patiti hydrothermal system is characterized by intense hydrothermal plumes and large heat-flux (de Ronde et al., this volume, Stucker et al., this volume, Tivey et al., this volume). Here heat-flux data up to 15 W/m^2 are aligned along a linear, southwest-northeast trend with the same orientation as the Tarawera Rift. Similarly, the surface expression of hydrothermal plumes (Fig. 2) follows the same orientation. No clear demagnetization anomaly is observed in this region, despite the clear indication of hydrothermal activity.

The 3-D magnetization model instead predicts a sharp, vertical contact between the demagnetized, hydrothermally altered unit in the northwest and the magnetized unit in the southeast, interpreted as fresh rhyolite. The boundary between these units forms a structural lineament with similar orientation as the Tarawera Rift and may represent the shallow expression of a vertical or sub-vertical fault providing a preferred pathway for the upflow of the hydrothermal fluids from a deep magmatic source (de Ronde et al., this volume; Mazot et al., 2014). This interpretation would explain the spatial orientation of the hydrothermal plumes and the shape of the heat-flow anomaly.

The absence of a well-defined demagnetization anomaly at the Patiti hydrothermal system clearly indicates that there is no significant volume of hydrothermally altered rocks relative to the Pink Terraces hydrothermal system. This discrepancy could be caused by two main factors. The hydrothermal flux could be relatively low in this region and/or the Patiti hydrothermal system is young and still developing so there has been insufficient time to alter a large volume of rock. However, the present-day heat-flow data and concentration of hydrothermal plumes indicate that the hydrothermal flux in this area is of a similar intensity to the northwest shore region, where we observe a well-defined demagnetization anomaly. This suggests that the more likely explanation is that the Patiti hydrothermal system was formed only recently and has not had enough time to create a well-defined demagnetization anomaly.

This interpretation confirms that the 1886 eruption changed the pre-existing hydrothermal setting at Lake Rotomahana causing the birth of a new hydrothermal system in this region (Simmons et al., 1993), along a structural lineament related to the Tarawera Rift. This would mean that the hydrothermal system has only been active for 130 years, which may simply be an insufficient time to hydrothermally alter a significant volume of rock. Given that there are similar hydrothermal fluxes at both sites, it is apparent that the Pink Terraces hydrothermal system represents a well-defined, old system which was well active before the 1886 eruption.

Estimating the time required to completely alter a significant volume of rock is a complex task as it depends on the intensity of the hydrothermal flux and its temporal variability among other factors. However, a rough estimate can be derived based on estimated time required to alter volcanics at other hydrothermal systems. At Poás volcano Rowe et al. (1992) estimated a rate of rock dissolution of ~1650 m^3/year. This is a small system compared to Nevado del Ruiz volcano, where Lopez and Williams (1993) estimated a rock dissolution rate up to 12600 m^3/year. Similarly, the dissolution rate at White Island reaches 22000 m^3/year (Giggenbach, 1987; Giggenbach and Sheppard, 1989).

The volume of demagnetized rocks at the northwestern lake shore hydrothermal site estimated from the model in Fig. 7 is ~10^8 m^3. Assuming that a similar volume of demagnetized rocks is needed to produce a similar demagnetization anomaly for the Patiti hydrothermal system, even using a dissolution rate of 50000 m^3/year (which is more than twice the value observed at White Island) it would take 2000 years to completely alter and demagnetize a corresponding volume of rock. These numbers not only suggest a young age for the hydrothermal activity west of Patiti Island, but also corroborate the hypothesis that the Pink Terraces hydrothermal system is old and definitely predates the 1886 eruption.

To fit some very intense, localized magnetic anomalies along the north shore and southwest shore of Lake Rotomahana a third highly magnetized rock unit (~10 A/m) is required in addition to fresh rhyolite rocks (modelled as 2.5 A/m magnetization) and hydrothermally altered rocks (modelled as 0 A/m magnetization). Some of these intense and localized magnetic anomalies are visible in Fig.4b close to the pre-1886 basalt outcrops.

Solidified basalts dikes in the TVZ typically have a magnetization of ~10 A/m (Soengkono, 2001; Rogan, 1982). Furthermore, shallow basalts under Lake Rotomahana are expected to produce large and sharply defined magnetic anomalies, typically associated with narrow dykes. Similar intense, localized magnetic anomalies have been observed along profiles across the Tarawera Rift and were interpreted as basalts at shallow depth by Cole and Hunt (1968). The magnetic model of Fig. 7 provides evidence of 6 possible basalt dikes, 5 are located along the northern side of Lake Rotomahana and one is located close to the southwestern lake shore above the sharp contact between the magnetized and demagnetized units (southernmost highly magnetic body in Fig. 7a).

In order to understand if these basalts were emplaced during the 1886 eruption we need additional information as magnetic data alone cannot be used to infer the age of the units. The 5 possible basalt dikes predicted from the model on the north shore of Lake Rotomahana are located 200-400 m away from the location of the Tarawera Rift as inferred from seismic data (de Ronde et al., this volume). Two of them are located close to a known pre-1886 basalt outcrop and probably pre-date the eruption. The remaining three are located near the boundary of the demagnetized body related to the pre-1886 hydrothermal system. Their relationship with the 1886 eruption of Mt Tarawera is equivocal because it is uncertain how much they would have been affected by the demagnetization effects of the long-lived hydrothermal system in that region.

The sixth possible basalt dike on the southwest shore of Lake Rotomahana is located over the sharp magnetization boundary interpreted as a structural lineament separating the Pink Terraces hydrothermal system and the volcanic unit (rhyolite) on the south lake shore. Most of the hydrothermal plume manifestations are located at the flanks of this body (Fig.4). If the associated structural lineament is related to the Tarawera Rift, then this basalt dike could have been emplaced during the 1886 eruption.

6. Conclusions

Gravity data at Lake Rotomahana clearly outline the subsidence associated with the Haroharo caldera that occurred 330 ka as part of the Matahina eruptive episode. This is wider than the previously mapped topographic expressions of the caldera margins. Inversion of regional aeromagnetic data suggests a large demagnetized body is located under the Waimangu Valley and extends east under the northwestern shore of Lake Rotomahana. This body is interpreted as a zone of demagnetization related to hydrothermal alteration and represents a deep connection between the Waimangu and Rotomahana portions of the Waimangu-Rotomahana-Mt Tarawera geothermal field.

Inversion of high-resolution magnetic data acquired on the lake shows a clear correlation between a demagnetized body under the Pink Terraces hydrothermal system, recently collected heat-flux data, and hydrothermal plumes, confirming that long term upflow and widespread hydrothermal alteration are the most likely explanations for this demagnetized region. The volume of hydrothermally altered rocks estimated by the volume of the demagnetized region suggests that this hydrothermal system was active before the 1886 eruption.

In contrast, no demagnetization anomaly is observed at the Patiti hydrothermal system, where there is high heat-flux and intense hydrothermal plume activity suggesting a strong hydrothermal system. In this region, magnetic and gravity data provide evidence of a structurally controlled fracturing, possibly fault or caldera boundary related. Activation is likely to have been generated by the 1886 eruption.

Locally, very intense and sharply-defined magnetic anomalies suggest the presence of basalt dikes, mainly located along the northwestern shore of Lake Rotomahana. The location of some of these suggests these basalts were emplaced before the 1886 eruption, however, the time of emplacement of others is equivocal because it is uncertain how much they would have been affected by the demagnetization effects of the long-lived hydrothermal system in that region. The intense and sharp magnetic anomaly interpreted as a basalt dike located close to the southwest lake shore, may be related to the structural lineament controlling the hydrothermal system in this region.

Acknowledgments:

The comments by Filippo Muccini and an unknown reviewer significantly improved the level of the paper. We thank the skipper of the Waikato University boat Dirk Immenga for the accurate navigation and successful operation of the magnetometer during the lake magnetic survey. We thank Harvey James of Waimangu Valley, Te Arawa Lakes Trust Board and the Bay of Plenty Regional Council for the logistical support. Science funding provided by GNS Science Strategic Development Fund.

REFERENCES

Bannister, S., Sherburne, S., Bourguignon, S., 2015. Earthquake swarm activity highlights a crustal fault associated with the Waimangu-Rotomahana-Mt Tarawera geothermal field, Taupo Volcanic Zone, New Zealand. This volume.

Bibby, H.M., Bennie, S.L., Stagpoole, V.M., Caldwell, T.G., 1994. Resistivity structure of the Waimangu, Waiotapu, Waikite and Reporoa Geothermal areas, New Zealand. Geothermics 23, 445-471.

Blakely, R. J., 1995. Potential Theory in Gravity and Magnetic Applications, Cambridge University Press, New York.

Caratori Tontini, F., Faggioni O., Beverini, N., Carmisciano, C., 2003. Gaussian envelope for 3D geomagnetic data inversion. Geophysics, 68, 996-1007.

Caratori Tontini, F., Graziano, F., Cocchi, L., Carmisciano, C., Stefanelli, P., 2007. Determining the optimal Bouguer density for a gravity data-set: implications for the isostatic setting of the Mediterranean Sea. Geophysical Journal International, 169, 380-388.

Caratori Tontini, F., Cocchi, L., Muccini, F., Carmisciano, C., Marani, M., Bonatti, E., Ligi, M., Boschi, E., 2010. Potential-field modelling of collapse-prone submarine volcanoes in the southern Tyrrhenian Sea (Italy). Geophysical Research Letters, 37, p. L03305, doi:10.1029/2009GL041757.

Caratori Tontini, F., Davy, B.W., de Ronde, C.E.J., Embley, R.W., Leybourne, M., Tivey, M.A., 2012a. Crustal magnetization of Brothers volcano, New Zealand, measured by autonomous underwater vehicles: geophysical expression of a submarine hydrothermal system. Economic Geology, 107, 1571-1581.

Caratori Tontini, F., de Ronde, C., Yoerger, D., Kinsey, J., Tivey, M., 2012b. 3-D focused inversion of near-seafloor magnetic data with application to the Brothers volcano hydrothermal system, Southern Pacific Ocean, New Zealand. Journal of Geophysical Research, 117, B10102, doi:10.1029/2012JB009349.

Caratori Tontini, F., de Ronde, C.E.J., Kinsey, J., Soule, A.S., Yoerger, D., Cocchi, L., 2013. Geophysical modeling of collapse-prone zones at Rumble III seamount, southern Pacific ocean, New Zealand. Geochemistry Geophysics Geosystems, doi: 10.1002/ggge.20278.

Carmichael, R.S., 1982. Magnetic properties of minerals and rocks. In: Carmichael, R.S. (Ed.), Handbook of Physical properties of Rocks, Vol. II. GRC Press, Boca Raton, FL, 229-287.

Cole, J.W., Hunt, T.M., 1968. Basalt dikes in the Tarawera Volcanic Complex, New Zealand. New Zealand Journal of Geology and Geophysics 11, 1203-1206.

Cole, J.W., 1970. Structure and eruptive history of the Tarawera Volcanic Complex. New Zealand Journal of Geology and Geophysics 13, 879-902.

Cox, A., 1971. Remanent magnetization and susceptibility of Late Cenozoic rocks from New Zealand. New Zealand Journal of Geology and Geophysics 14, 192, 207.

Darragh, M., Cole, J.W., Nairn, I.A., Shane, P., 2006. Pyroclastic stratigraphy and eruption dynamics of the 21.9 ka Okareka and 17.6 ka Rerewhakaaitu eruption episode from Tarawera Volcano, Okataina Volcanic Centre, New Zealand. Journal of Geophysical Research 34, 8221-8232.

Davy, B.W., Caldwell, T.G., 1998. Gravity, magnetic and seismic surveys of the Caldera complex, Lake Taupo, North Island, New Zealand. Journal of Volcanology and Geothermal Research 81, 69-89.

Davy, B.W., Bibby, H., 2005. Seismic reflection imaging of the Haroharo Caldera boundary beneath Lake Tarawera, Okataina Volcanic Center, New Zealand. New Zealand Journal of Geology and Geophysics 48, 153-166.

de Ronde, C.E.J., Walker, S.L., LeBlanc, C., Davy, B.W., Fornari, D.J., Caratori Tontini, F., Scott, B.J., Seebeck, F.H., Stewart, T., Mazot, A., Nicol, A., Tivey, M.A., 2015. Reconstruction of the geology and structure of Lake Rotomahana and its hydrothermal systems from high-resolution multibeam mapping and seismic surveys: Effects of the 1886 Mt. Tarawera eruption. This volume.

Faggioni, O., Caratori Tontini, F., 2002. Quantitative evaluation of the time-line reduction performance in high definition marine magnetic surveys: Marine Geophysical Researches, 23, 353-365.

Finlay, C.C, Maus, S., Beggan, C.D., Bondar, T.N., Chambodut, A., Chernova, T.A., Chulliat, A., Golovkov, V.P., Hamilton, B., Hamoudi, M., Holme, R., Hulot, G., Kuang, W., Langlais, B., Lesur, V., Lowes, F.J., Lühr, H., Macmillan, S., Mandea, M., McLean, S., Manoj, C., Menvielle, M., Michaelis, I., Olsen, N., Rauberg, J., Rother, M., Sabaka, T.J., Tangborn, A., Tøffner-Clausen, L., Thébault, E., Thomson, A.W.P., Wardinski, I., Wei, Z., Zvereva, T.I., 2010. International Geomagnetic Reference Field: the eleventh generation. Geophysical Journal International, 183, 1216-1230.

Giggenbach, W.F., 1987. Redox processes governing the chemistry of fumarolic gas discharges from White Island, New Zealand. Applied Geochemistry 2, 143-161.

Giggenbach, W.F., Sheppard, D.S., 1989. Variations in the temperature and chemistry of White Island fumarole discharges 1972-85. New Zealand Geological Survey Bulletin 103, 119-126.

Hatherton, T., Leopard, A.E., 1964. The densities of New Zealand rocks. New Zealand Journal of Geology and Geophysics 7, 605-625.

Healy, J. 1975a. Volcanic lakes. Pp 70-83 in Jolly, V.H.; Brown, J.M.A. (Eds): New Zealand Lakes. Auckland University Press.

Healy, J. 1975b. The gross effects of rainfall on lake levels in the Rotorua District. Journal of Royal Society of New Zealand 5: 77-100.

Heise, W., Caldwell, T.G., Bertrand, E.A., Hill, G.J., Bennie, S.L., Palmer, N.G., 2015. Imaging the deep source of the Rotorua and Waimangu geothermal fields, Taupo Volcanic Zone, New Zealand.

Hochstein, M.P., Hunt, T., 1970. Seismic, gravity and magnetic studies: Broadlands Geothermal Field. Geothermics, Spec. Ed. 2, 333-346.

Hochstein, M.P., Soengkono, S., 1997. Magnetic anomalies associated with high temperature reservoirs in the Taupo volcanic zone (New Zealand). Geothermics 26, 1-24.

Hochstetter, F. Von, 1864. Geologie vone Neu Zealand. Vienna. (Translated by C.A. Fleming 1959). Government Printer, Wellington.

Keam, R.F., 1988. The volcanic eruption of 10 June 1886. A comprehensive account. Tarawera. R.F. Keam, New Zealand.

Keam, R., 2015. The Tarawera eruption, Lake Rotomahana, and the origin of the Pink and White Terraces. This volume.

Leonard, G.S.; Begg, J.G.; Wilson, C.J.N. (comps) 2010 Geology of the Rotorua area: scale 1:250,000. Lower Hutt: GNS Science. Institute of Geological & Nuclear Sciences 1:250,000 geological map 5. 102 p. + 1 folded map.

Leonard, G.S., Cole, J.W., Nairn, I.A., Self, S., 2002. Basalt triggering the c. AD 1305 Kaharoa rhyolite eruption, Tarawera Volcanic Complex, New Zealand. Journal of Volcanology and Geothermal Research 115, 461-486.

Lindgren, 1933. Mineral Deposits, 4th Edition. McGraw-Hill, New York.

Lopez, D.L., Williams, S.N., 1993. Catastrophic volcanic collapse: relation to hydrothermal processes. Science 260, 1794-1796.

Malahoff, A., 1968. Origin of magnetic anomalies over the Central Volcanic Region of New Zealand. In: Knopoff, L., Drake, C.L., Hart, P.J., The Crust and Upper Mantle of the Pacific Area, Geophysical Monograph Series v.12, AGU, Washington DC, 218-240.

Mazot, A., Schwander, F.M., Christenson, B., de Ronde, C.E.J., Inguaggiato, S., Scott, B., Graham, D., Britten, K., Keeman, J., Tan, K., 2014. CO2 discharge from the bottom of volcanic Lake Rotomahana, New Zealand. Geochemistry, Geophysics, Geosystems 15, 577-588, doi:10.1002/2013GC004945.

Nairn, I.A., 1979. Rotomahana-Waimangu eruption, 1886: base surge and basalt magma. New Zealand Journal of Geology and Geophysics 22, 363-378.

Nairn, I.A., 1981. Some studies of the geology, volcanic history and geothermal resources of the Okataina Volcanic Center, Taupo Volcanic Zone, New Zealand. Unpublished Ph.D. thesis, lodged in the library, Victoria University of Wellington.

Nairn, I.A., Cole, J.W., 1981. Basalt dikes in the 1886 Tarawera Rift. New Zealand Journal of Geology and Geophysics 24, 585-592.

Nairn, I.A., 1989. Mount Tarawera. Geological map of New Zealand 1:50000. Map 1 sheet and notes. Wellington, New Zealand, Department of Scientific and Industrial Research.

Nairn, I.A., 1992. The Te Rere and Okareka eruption episodes – Okataina Volcanic Centre, Taupo Volcanic Zone, New Zealand. New Zealand Journal of Geology and Geophysics 35, 93-108.

Nairn, I.A. 2002 Geology of the Okataina Volcanic Centre: sheets part U15, part U16, part V15 & part V16, scale 1:50,000. Lower Hutt: Institute of Geological & Nuclear Sciences. Institute of Geological & Nuclear Sciences geological map 25. 156 p. + 1 fold map.

Rogan, A.M., 1982. A geophysical study of the Taupo Volcanic Zone, New Zealand. Journal of Geophysical Research 87, 4073-4088.

Rogan, M., Hochstein, M.P., 1984. Magnetic survey of the 1886 Tarawera Rift. New Zealand Journal of Geology and Geophysics 27, 237-245.

Rowe, G.L., Brantley, S.L., Fernandez, M., Fernandez, J.F., Borgia, A., Barquero, J., 1992. Fluid-volcano interaction in an active stratovolcano: the crater lake system of Poás volcano, Costa Rica. Journal of Volcanology and Geothermal Research, 49, 23-51.

Seebeck, H., Nicol, A., Stern, T.A., Bibby, H.M., Stagpoole, V.M., 2010. Fault controls on the geometry and location of the Okataina Caldera, Taupo Volcanic Zone, New Zealand. Journal of Volcanology and Geothermal Research 190, 136-151.

Shane, P., Martin, S.B., Smith, V.C., Beggs, K.F., Darragh, M.B., Cole, J.W., Nairn, I.A., 2007. Multiple rhyolite magmas and basalt injection in the 17.7 ka Rerewhakaaitu eruption episode from Tarawera volcanic complex, New Zealand. Journal of Volcanology and Geothermal Research 164, 1-26.

Silva, J.B.C., Medeiros, W.E., Barbosa, V.C.F., 2001. Potential-field inversion: Choosing the appropriate technique to solve a geological problem. Geophysics, 66, 511–520.

Simmons, S.F., Keywood, Scott, B.J., Keam, R.F., 1993. Irreversible change of the Rotomahana-Waimangu system (New Zealand) as a consequence of a volcanic eruption. Geology 21, 643-646.

Stagpoole, V., 1994. Interpretation of refraction seismic and gravity data across the Eastern margin of the Taupo Volcanic Zone, New Zealand. Geothermics 23, 501-510.

Stagpoole, V., Bibby, H.M., 1999. Residual gravity anomaly of the Taupo Volcanic Zone, New Zealand, 1:250000. Institute of Geological and Nuclear Sciences Geophysical Map 13. Institute of Geological and Nuclear Sciences Ltd, Lower Hutt, New Zealand.

Stern, T.A., 1979. Regional and residual gravity fields, central North Island, New Zealand. New Zealand Journal of Geology and Geophysics 22, 479-485.

Stern, T.A., 1986. Geophysical studies of the upper crust within the central volcanic region, New Zealand. In: Smith, I.E.M. (Ed.), Cenozoic Volcanism: Royal Society of New Zealand Bulletin, 23, 92-111.

Soengkono, S., 1995. A magnetic model for deep plutonic bodies beneath the central Taupo volcanic zone, North Island, New Zealand. Journal of Volcanology and Geothermal Research 68, 193-207.

Soengkono, S., 2001. Interpretation of magnetic anomalies over the Waimangu geothermal area, Taupo volcanic zone, New Zealand. Geothermics 30, 443-459.

Stucker, V.K., de Ronde, C.E.J., Scott, B.J., Wilson, N.J., Walker, S.L., Lupton, J.E., 2015. Subaerial and sublacustrine hydrothermal activity at Lake Rotomahana. This volume.

Tivey, M.A., Johnson, H.P., 2002. Crustal magnetization reveals subsurface structure of Juan de Fuca Ridge hydrothermal vent fields. Geology, 30, 979–982.

Tivey, M.A., Dyment, J., 2010. The magnetic signature of hydrothermal systems in slow spreading environments. In: Rona, P., Devey, C., Murton, B., Diversity of hydrothermal systems on slow spreading ocean ridges, Geophysical Monograph Series v.188, AGU, Washington DC, 43-65.

Tivey, M.A., de Ronde, C.E.J., Caratori Tontini, F., Walker, S., Fornari, D. A novel heat flux study of a geothermally active lake – Lake Rotomahana, New Zealand. This volume.

Villamor, P., Nairn, I.A., Seebeck, H., 2007. Fieldtrip 2: earthquakes and eruptions at Okataina Volcanic Centre. In: Cochran, U.A.; Cervelli, A. (comps) Geological Society of New Zealand & New Zealand Geophysical Society Joint Annual Conference: launching International Year of Planet Earth, 26-29 November 2007, Tauranga: fieldtrip guides. Geological Society of New Zealand miscellaneous publication 123B, 7-27.

Walker, G.P.L., Self, S., Wilson, L., 1984. Tarawera 1886, New Zealand – a basaltic plinian fissure eruption. Journal of Volcanology and Geothermal Research 21, 61-78.

Walker, S.L., de Ronde, C.E.J., Fornari, D., Tivey, M.A., Stucker, V., 2015. High-resolution water column survey to identify active sublacustrine hydrothermal discharge zones within Lake Rotomahana, North Island, New Zealand. This volume.

Whiteford, P.C., Graham, D.J., 1995. Conductive heat flow through the sediments in Lake Rotomahana, New Zealand. Geothermics 23, 527-538.

Wilson, C.J.N., Rogan, A.M., Smith, I.E.M., Northey, D.J., Nairn, I.A., Houghton, B.F., 1984. Caldera Volcanoes of the Taupo Volcanic Zone, New Zealand. Journal of Geophysical Research 89, 8463-8484.

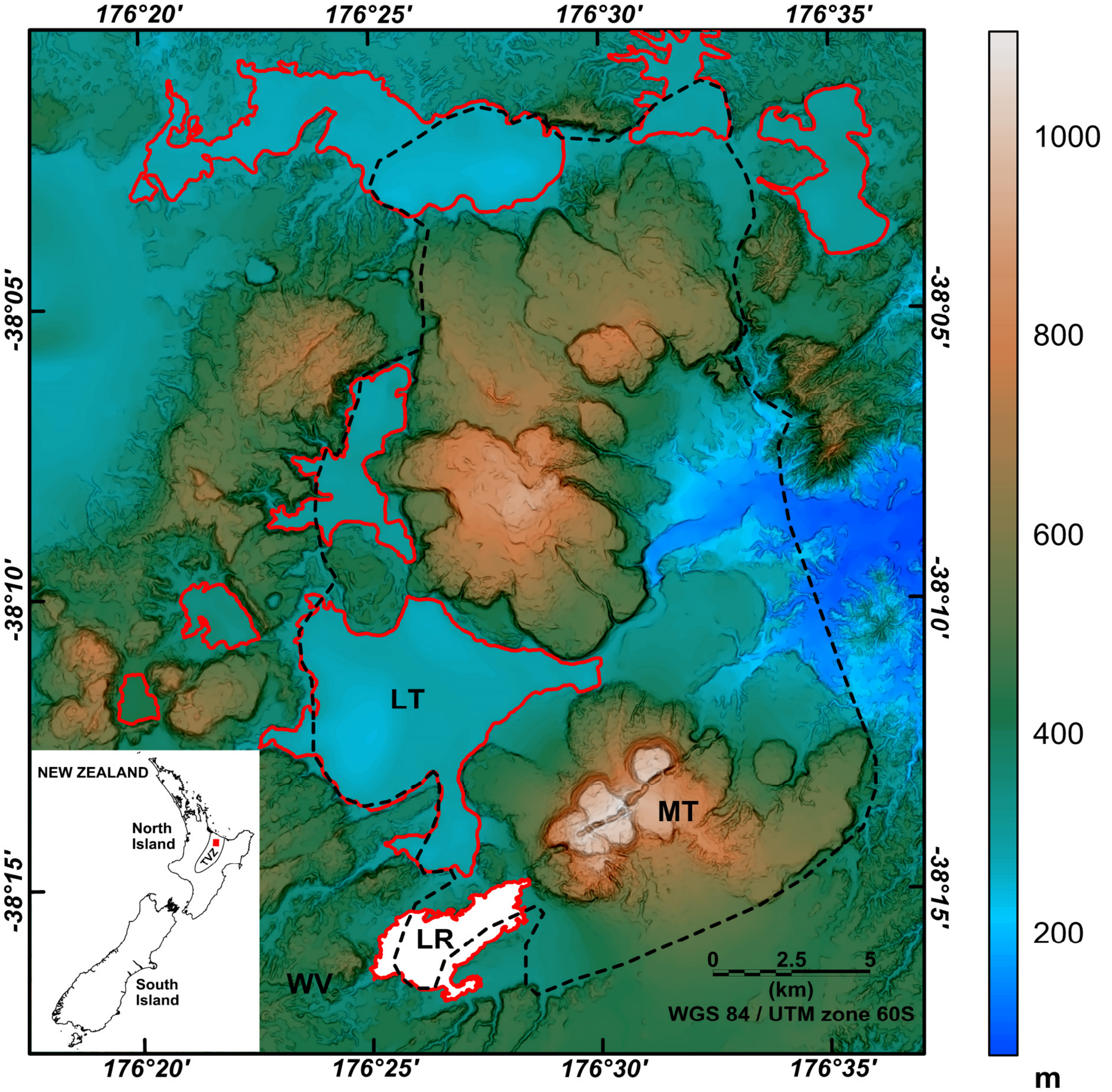

Fig.1: Map showing the location of Lake Rotomahana (LR) relative to Haroharo Caldera (black dashed line) in the Okataina Volcanic Center. The 1886 Tarawera Rift along Mt Tarawera (MT) is clearly visible extending through Lake Rotomahana to the Waimangu Valley (WV). The red polygons mark the boundaries of the Rotorua Lakes; Lake Tarawera (LT) is located 1 km North of Lake Rotomahana (filled in white). The inset shows the location of the Rotorua Lakes area (red rectangle) within the Taupo Volcanic Zone (TVZ).

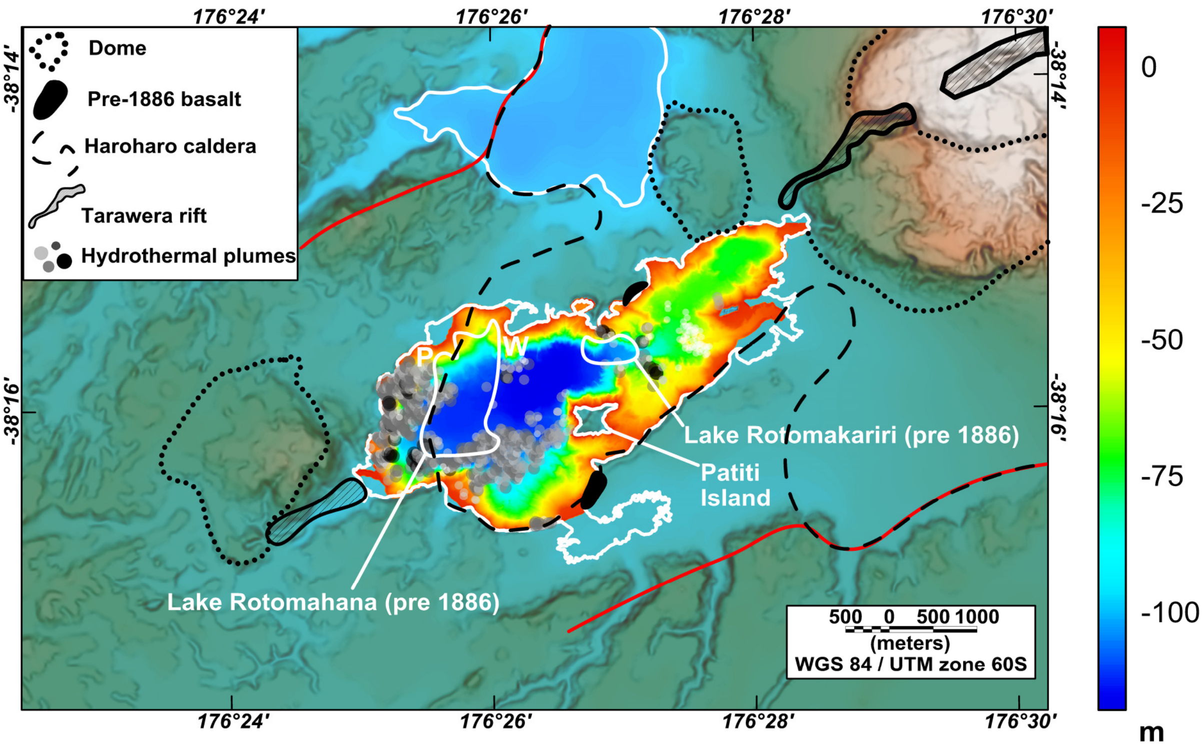

Fig.2: Map showing the Lake Rotomahana bathymetry (de Ronde et al., this issue) with location of structural lineaments and geological outcrops. The circles show the location of hydrothermal plumes, with sizes proportional to the activity and greyscale colours from light (low activity) to dark (high activity). The positions of the pre-1886 lakes (Rotomahana and Rotomakariri) and the Pink and White Terraces (P and W, respectively) are also shown. The red line is the gravity-derived caldera boundary (see Figure 5).

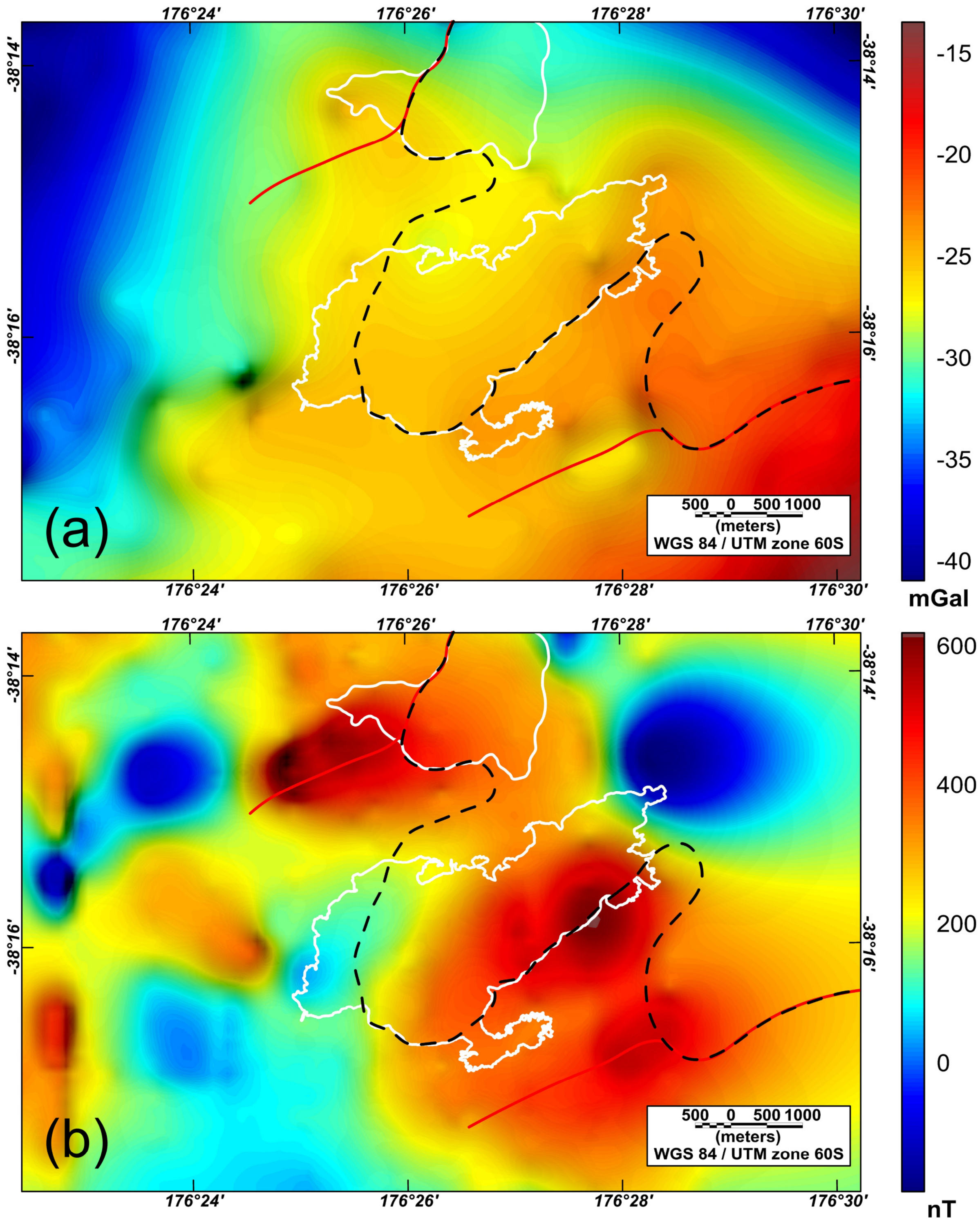

Fig.3: Geophysical maps of Lake Rotomahana. (a) Residual Bouguer gravity anomaly map derived by the subtraction of the regional field of Stern (1979). (b) Aeromagnetic map (Soengkono, 2001). Red line and black dashed line indicate the gravity-derived and topographic caldera boundaries, respectively (see Figure 5).

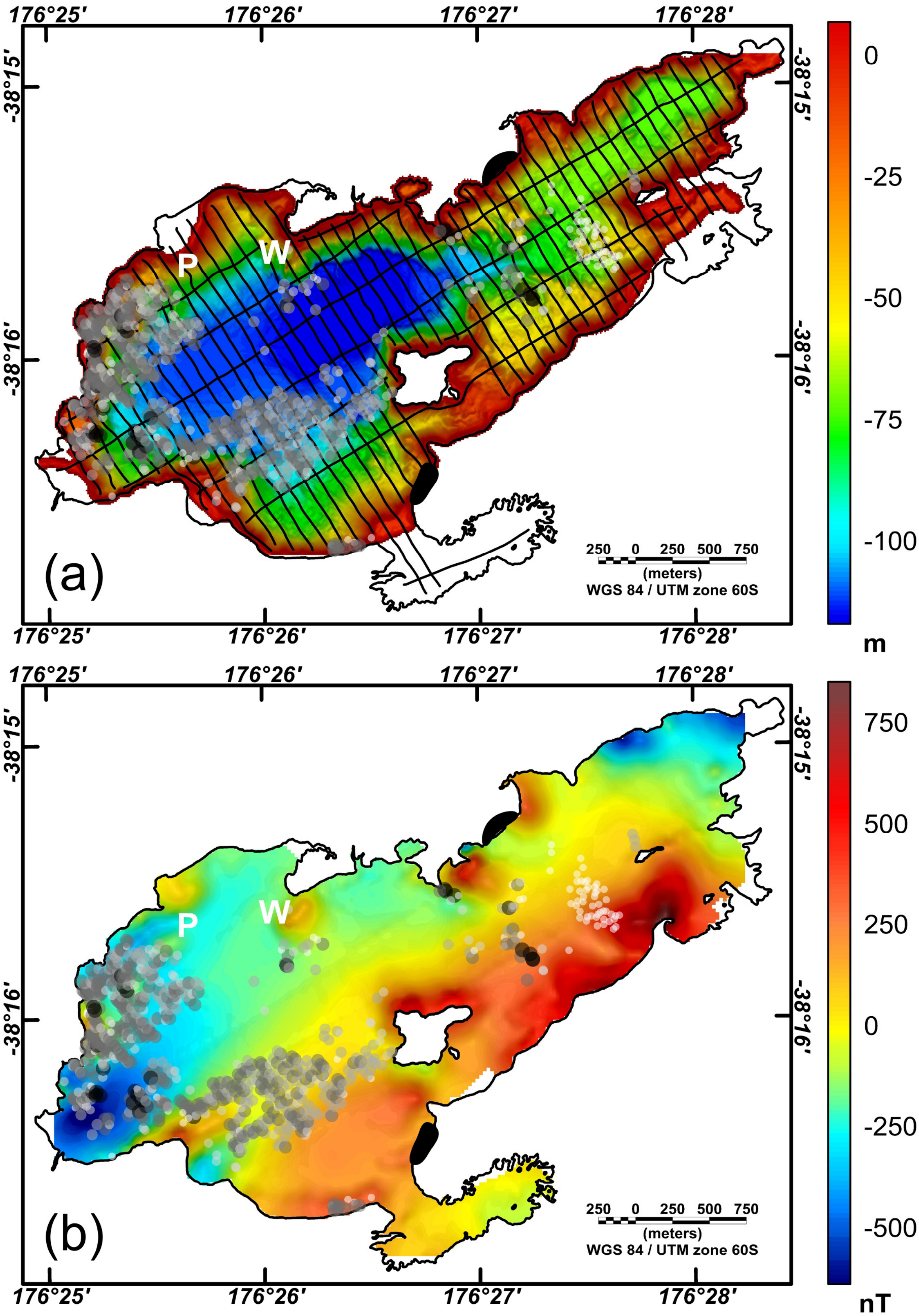

Fig.4: Magnetic survey of Lake Rotomahana, with locations of pre-1886 basalt outcrops and hydrothermal plumes (see Fig.2). (a) Survey lines overlying the bathymetry. (b) Magnetic anomaly map (TMI). P and W are the approximate location of the Pink and White terraces.

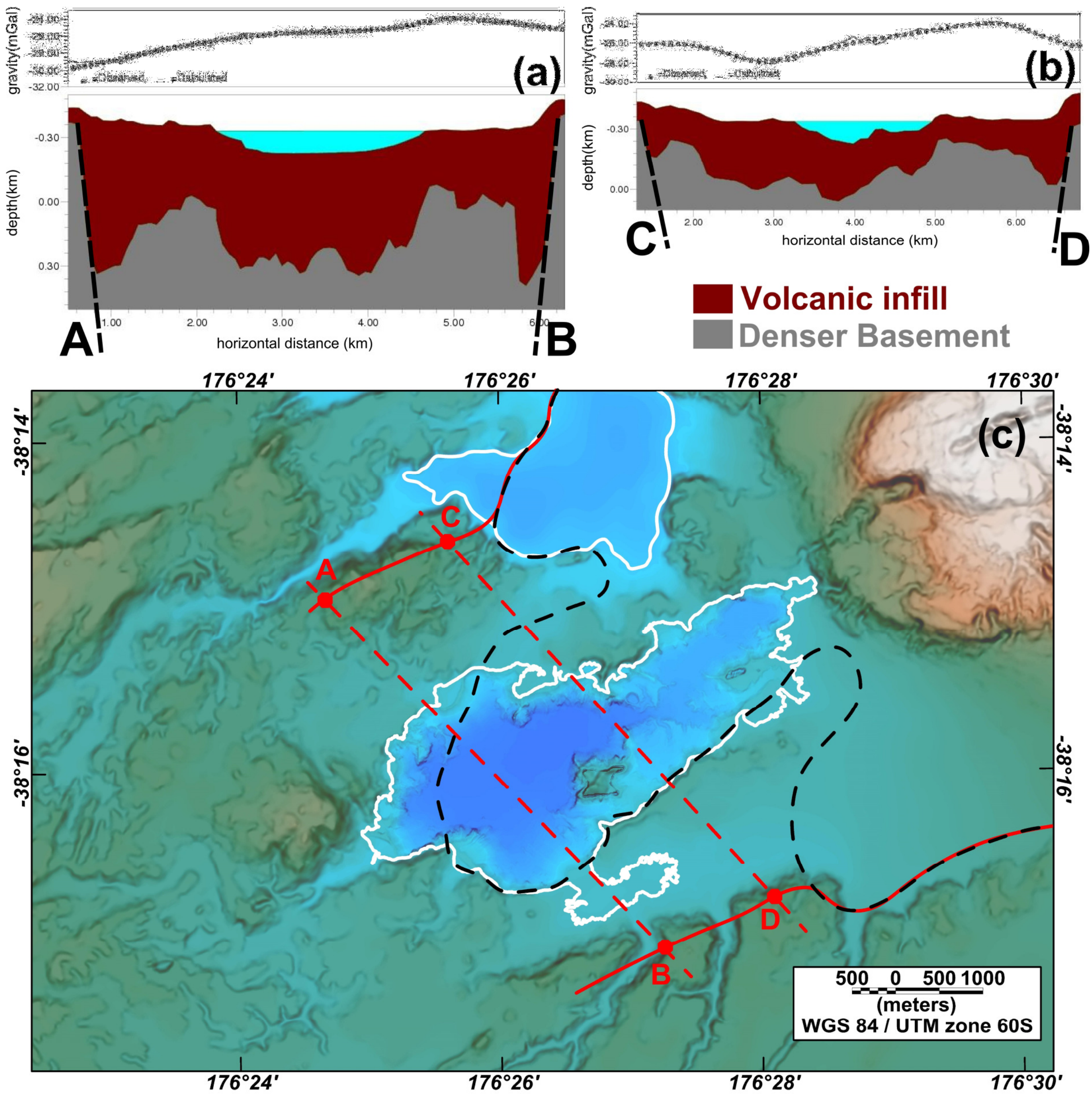

Fig.5: Section gravity model. Volcanic infill density is 2.17 g/cm^3 and basement density is 2.67 g/cm^3 (a) First section, A-B in Fig.5c. (b) Second section, C-D in Fig.5c. (c) Location of gravity sections and inferred caldera boundary (red line).

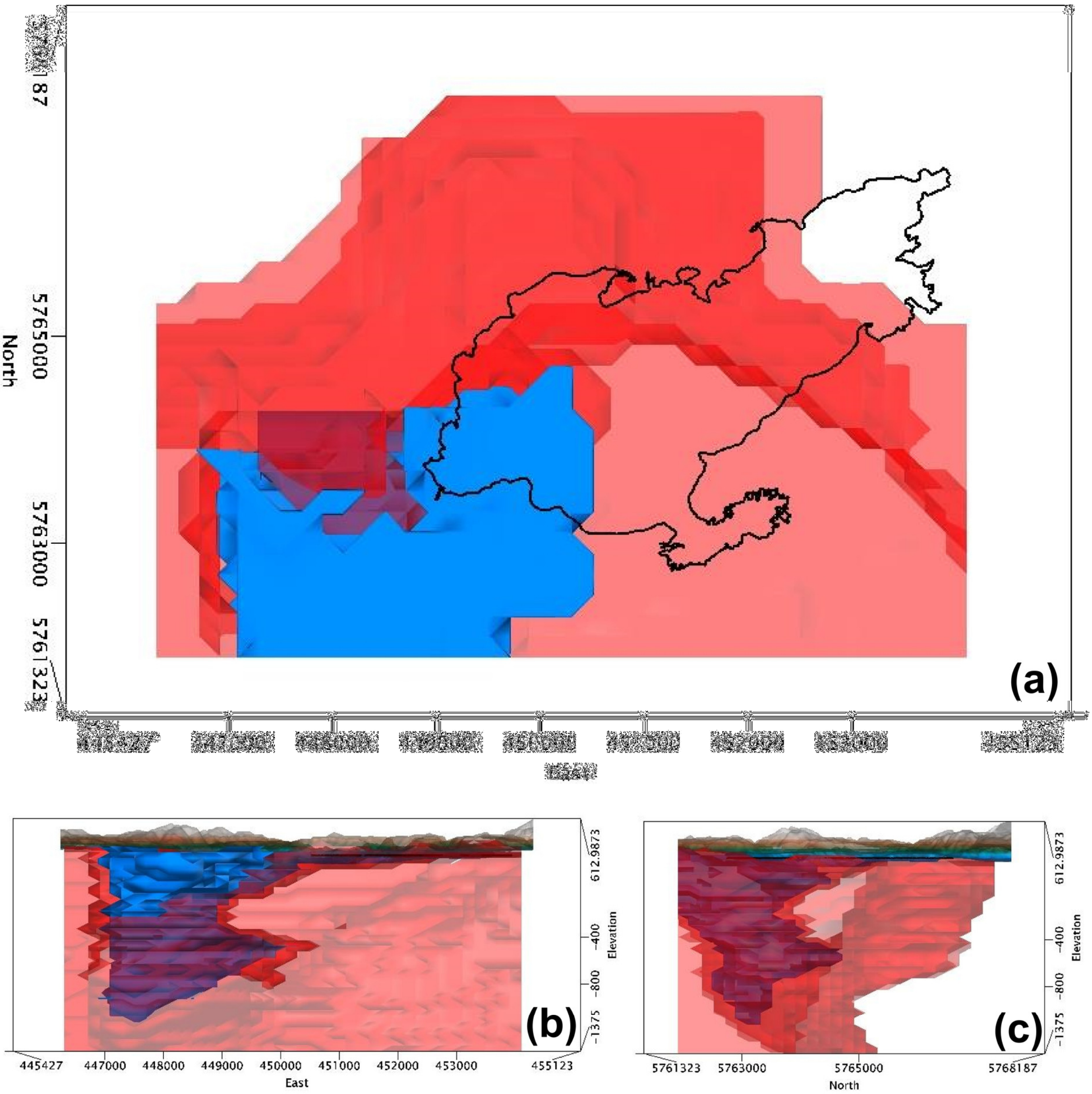

Fig.6: Aeromagnetic data inversion model (vertical exaggeration 2x). The blue and red isosurfaces enclose demagnetized (0 A/m) and magnetized rocks (2.5 A/m), respectively. (a) Perspective view from top. (b) Perspective view from south. (c) Perspective view from east.

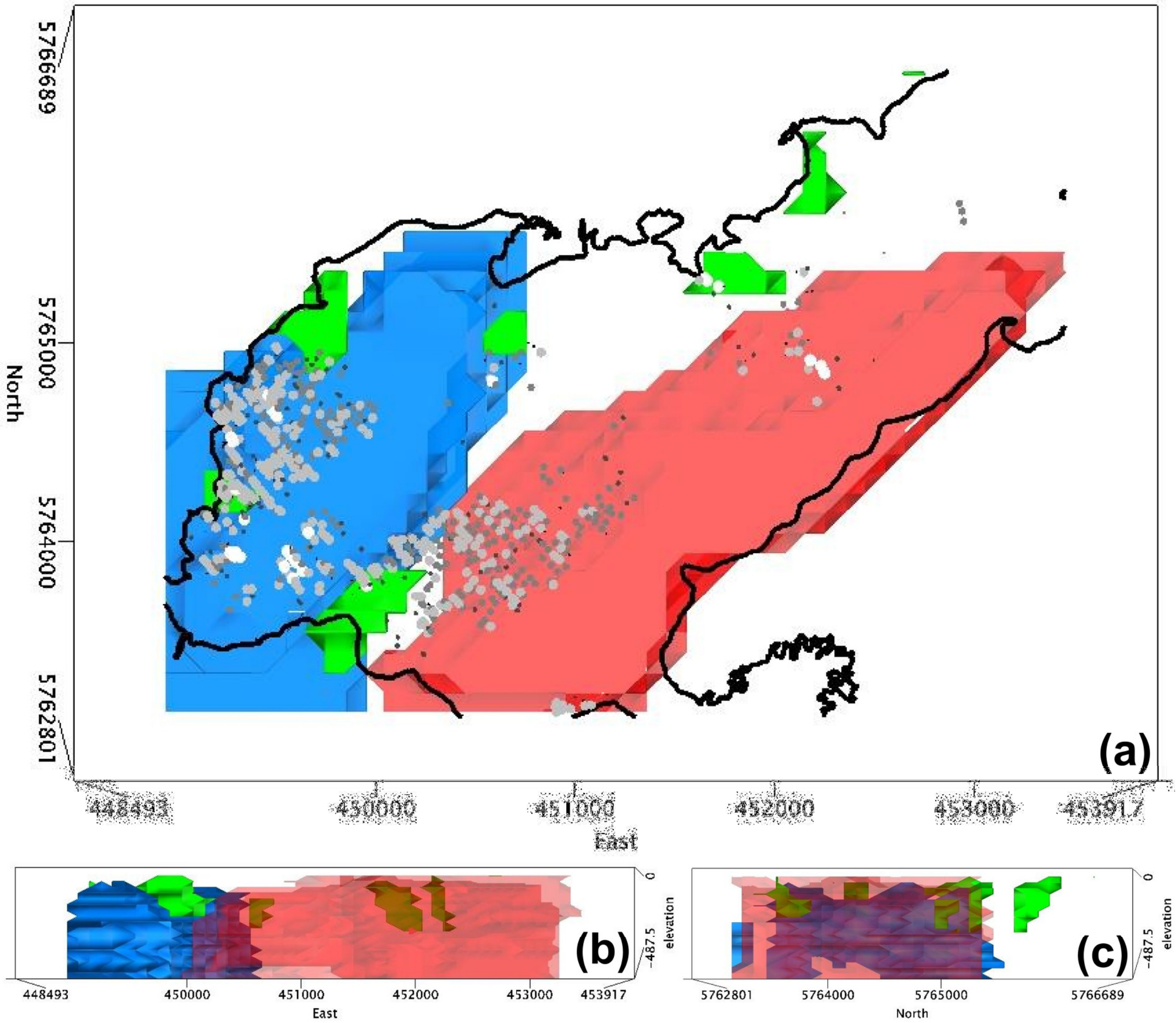

Fig.7: Lake magnetic data inversion model (vertical exaggeration 2x) with surface locations of hydrothermal plumes (see Fig. 2). The blue and red isosurfaces enclose demagnetized (0 A/m) and magnetized rocks (2.5 A/m), respectively. The green isosurfaces enclose highly magnetized rocks (10 A/m). (a) Perspective view from top. (b) Perspective view from south. (c) Perspective view from east.